Gold nanoparticles as a saturable absorber for visible 635 nm Q-switched pulse generation

Article *in* Optics Express · September 2015

DOI: 10.1364/OE.23.024071

7 authors, including:

Zhiping Cai
Xiamen University
361 PUBLICATIONS **3,066** CITATIONS
SEE PROFILE

Jian Weng
Xiamen University
77 PUBLICATIONS **1,458** CITATIONS
SEE PROFILE

Zhengqian Luo
Xiamen University
80 PUBLICATIONS **964** CITATIONS
SEE PROFILE

Huiying Xu
Xiamen University
134 PUBLICATIONS **1,035** CITATIONS
SEE PROFILE

Gold nanoparticles as a saturable absorber for visible 635 nm Q-switched pulse generation

Duanduan Wu,[1] Jian Peng,[2] Zhiping Cai,[1,*] Jian Weng,[2] Zhengqian Luo,[1] Nan Chen,[1] and Huiying Xu[1]

[1]*Institute of Optoelectronic Technology, Department of Electronic Engineering, Xiamen University, Xiamen 361005, China*

[2]*Department of Biomaterials, College of Materials, Xiamen University, Xiamen 361005, China*

[*]*zpcai@xmu.edu.cn*

Abstract: Gold nanoparticle (GNP) possesses saturable absorption bands in the visible region induced by surface plasmon resonance (SPR). We firstly applied the GNP as a visible saturable absorber (SA) for the red Q-switched pulse generation. The GNPs were embedded in polyvinyl alcohol (PVA) for film-forming and inserted into a praseodymium (Pr^{3+})-doped fiber laser cavity to achieve 635 nm passive Q-switching. The visible 635 nm Q-switched fiber laser has a wide range of pulse-repetition-rate from 285.7 to 546.4 kHz, and a narrow pulse width of 235 ns as well as the maximum output power of 11.1 mW. The results indicate that the GNPs-based SA is available for pulsed operation in the visible spectral range.

OCIS codes: (140.3540) Lasers, Q-switched; (140.7300) Visible lasers; (060.3510) Lasers, fiber.

References and links

1. Q. Bao, H. Zhang, Y. Wang, Z. Ni, Y. Yan, Z. X. Shen, K. P. Loh, and D. Y. Tang, "Atomic-layer graphene as a saturable absorber for ultrafast pulsed lasers," Adv. Funct. Mater. **19**(19), 3077–3083 (2009).
2. Z. Luo, M. Zhou, J. Weng, G. Huang, H. Xu, C. Ye, and Z. Cai, "Graphene-based passively Q-switched dual-wavelength erbium-doped fiber laser," Opt. Lett. **35**(21), 3709–3711 (2010).
3. D. D. Wu, Z. Q. Luo, F. F. Xiong, C. K. Zhang, Y. Z. Huang, S. S. Chen, W. W. Cai, Z. P. Cai, and H. Y. Xu, "Passive synchronization of 1.06- and 1.53-m fiber lasers Q-switched by a common graphene SA," IEEE Photonics Technol. Lett. **26**, 1474–1477 (2014).
4. I. H. Baek, H. W. Lee, S. Bae, B. H. Hong, Y. H. Ahn, D. I. Yeom, and F. Rotermund, "Efficient mode-locking of sub-70-fs Ti: sapphire laser by graphene saturable absorber," Appl. Phys. Express **5**(3), 032701 (2012).
5. G. R. Lin and Y. C. Lin, "Directly exfoliated and imprinted graphite nano-particle saturable absorber for passive mode-locking erbium-doped fiber laser," Laser Phys. Lett. **8**(12), 880–886 (2011).
6. Z. Sun, T. Hasan, F. Torrisi, D. Popa, G. Privitera, F. Wang, F. Bonaccorso, D. M. Basko, and A. C. Ferrari, "Graphene mode-locked ultrafast laser," ACS Nano **4**(2), 803–810 (2010).
7. J. Sotor, G. Sobon, and K. M. Abramski, "Sub-130 fs mode-locked Er-doped fiber laser based on topological insulator," Opt. Express **22**(11), 13244–13249 (2014).
8. Z. C. Luo, M. Liu, H. Liu, X. W. Zheng, A. P. Luo, C. J. Zhao, H. Zhang, S. C. Wen, and W. C. Xu, "2 GHz passively harmonic mode-locked fiber laser by a microfiber-based topological insulator saturable absorber," Opt. Lett. **38**(24), 5212–5215 (2013).
9. Y. H. Lin, C. Y. Yang, J. H. Liou, C. P. Yu, and G. R. Lin, "Using graphene nano-particle embedded in photonic crystal fiber for evanescent wave mode-locking of fiber laser," Opt. Express **21**(14), 16763–16776 (2013).
10. Y. H. Lin, Y. C. Chi, and G. R. Lin, "Nanoscale charcoal powder induced saturable absorption and mode-locking of a low-gain erbium-doped fiber-ring laser," Laser Phys. Lett. **10**(5), 055105 (2013).
11. S. Wang, H. Yu, H. Zhang, A. Wang, M. Zhao, Y. Chen, L. Mei, and J. Wang, "Broadband few-layer MoS_2 saturable absorbers," Adv. Mater. **26**(21), 3538–3544 (2014).
12. D. Mao, Y. Wang, C. Ma, L. Han, B. Jiang, X. Gan, S. Hua, W. Zhang, T. Mei, and J. Zhao, "WS_2 mode-locked ultrafast fiber laser," Sci. Rep. **5**, 7965 (2015).
13. Y. H. Lin, S. F. Lin, Y. C. Chi, C. L. Wu, C. H. Cheng, W. H. Tseng, J. H. He, C. Wu, C. K. Lee, and G. R. Lin, "Using n- and p-type Bi_2Te_3 topological insulator nanoparticles to enable controlled femtosecond mode-locking of fiber lasers," ACS Photonics **2**(4), 481–490 (2015).
14. H. Zhang, S. B. Lu, J. Zheng, J. Du, S. C. Wen, D. Y. Tang, and K. P. Loh, "Molybdenum disulfide (MoS_2) as a broadband saturable absorber for ultra-fast photonics," Opt. Express **22**(6), 7249–7260 (2014).
15. C. Zhao, Y. Zou, Y. Chen, Z. Wang, S. Lu, H. Zhang, S. Wen, and D. Tang, "Wavelength-tunable picoseconds soliton fiber laser with Topological Insulator: Bi_2Se_3 as a mode locker," Opt. Express **20**(25), 27888–27895 (2012).

#246394 Received 20 Jul 2015; revised 20 Aug 2015; accepted 21 Aug 2015; published 4 Sep 2015

16. H. I. Elim, J. Yang, J. Y. Lee, J. Mi, and W. Ji, "Observation of saturable and reverse-saturable absorption at longitudinal surface plasmon resonance in gold nanorods," Appl. Phys. Lett. **88**(8), 083107 (2006).
17. T. Jiang, Y. Xu, Q. J. Tian, L. Liu, Z. Kang, R. Y. Yang, G. S. Qin, and W. P. Qin, "Passively Q-switching induced by gold nanocrystals," Appl. Phys. Lett. **101**(15), 151122 (2012).
18. K. H. Kim, U. Griebner, and J. Herrmann, "Theory of passive mode locking of solid-state lasers using metal nanocomposites as slow saturable absorbers," Opt. Lett. **37**(9), 1490–1492 (2012).
19. K. H. Kim, U. Griebner, and J. Herrmann, "Theory of passive mode-locking of semiconductor disk lasers in the blue spectral range by metal nanocomposites," Opt. Express **20**(15), 16174–16179 (2012).
20. Z. Kang, Y. Xu, L. Zhang, Z. X. Jia, L. Liu, D. Zhao, Y. Feng, G. S. Qin, and W. P. Qin, "Passively mode-locking induced by gold nanorods in erbium-doped fiber lasers," Appl. Phys. Lett. **103**(4), 041105 (2013).
21. Z. Kang, X. Y. Guo, Z. X. Jia, Y. Xu, L. Liu, D. Zhao, G. S. Qin, and W. P. Qin, "Gold nanorods as saturable absorbers for all-fiber passively Q-switched erbium-doped fiber laser," Opt. Mater. Express **3**(11), 1986–1991 (2013).
22. Z. Kang, X. J. Gao, L. Zhang, Y. Feng, G. S. Qin, and W. P. Qin, "Passively mode-locked fiber lasers at 1039 and 1560 nm based on a common gold nanorod saturable absorber," Opt. Mater. Express **5**(4), 794–801 (2015).
23. X.-D. Wang, Z.-C. Luo, H. Liu, M. Liu, A.-P. Luo, and W.-C. Xu, "Microfiber-based gold nanorods as saturable absorber for femtosecond pulse generation in a fiber laser," Appl. Phys. Lett. **105**(16), 161107 (2014).
24. H. B. Liao, R. F. Xiao, J. S. Fu, P. Yu, G. K. L. Wong, and P. Sheng, "Large third-order optical nonlinearity in Au: SiO_2 composite films near the percolation threshold," Appl. Phys. Lett. **70**(1), 1–3 (1997).
25. K. H. Kim, A. Husakou, and J. Herrmann, "Linear and nonlinear optical characteristics of composites containing metal nanoparticles with different sizes and shapes," Opt. Express **18**(7), 7488–7496 (2010).
26. H. Baida, D. Mongin, D. Christofilos, G. Bachelier, A. Crut, P. Maioli, N. Del Fatti, and F. Vallée, "Ultrafast nonlinear optical response of a single gold nanorod near its surface plasmon resonance," Phys. Rev. Lett. **107**(5), 057402 (2011).
27. K. Tiwari, A. K. Singh, and S. C. Sharma, "Evidence for surface plasmons in a liquid crystal containing gold nanoparticles," Appl. Phys. Lett. **101**(25), 253103 (2012).
28. I. Cohanoschi, A. Thibert, C. Toro, S. L. Zou, and F. E. Hernandez, "Surface plasmon enhancement at a liquid-metal-liquid interface," Plasmonics **2**(2), 89–94 (2007).
29. W. P. McConnell, J. P. Novak, L. C. Brousseau, R. R. Fuierer, R. C. Tenent, and D. L. Feldheim, "Electronic and optical properties of chemically modified metal nanoparticles and molecularly bridged nanoparticle arrays," J. Phys. Chem. B **104**(38), 8925–8930 (2000).
30. G. Ma, W. Sun, S. H. Tang, H. Zhang, Z. Shen, and S. Qian, "Size and dielectric dependence of the third-order nonlinear optical response of Au nanocrystals embedded in matrices," Opt. Lett. **27**(12), 1043–1045 (2002).
31. Y. Yang, M. Nogami, J. Shi, H. Chen, G. Ma, and S. Tang, "Controlled surface-plasmon coupling in SiO_2-coated gold nanochains for tunable nolinear optical properties," Appl. Phys. Lett. **88**(8), 081110 (2006).
32. T. J. Norman, Jr., C. D. Grant, D. Magana, J. Z. Zhang, J. Liu, D. Cao, F. Bridges, and A. Van Buuren, "Near infrared optical absorption of gold nanoparticle aggregates," J. Phys. Chem. B **106**(28), 7005–7012 (2002).
33. S. Yamashita, "A tutorial on nonlinear photonic applications of carbon nanotube and graphene," J. Lightwave Technol. **30**(4), 427–447 (2012).
34. X. Zhu and N. Peyghambarian, "High-power ZBLAN glass fiber lasers: review and prospect," Adv. Optoelectron. **2010**, 501956 (2010).
35. H. Okamoto, K. Kasuga, I. Hara, and Y. Kubota, "Visible-NIR tunable Pr^{3+}-doped fiber laser pumped by a GaN laser diode," Opt. Express **17**(22), 20227–20232 (2009).
36. J. Peng, J. Weng, L. Ren, and L.-P. Sun, "Interactions between gold nanoparticles and amyloid β 25-35 peptide," IET Nanobiotechnol. **8**(4), 295–303 (2014).
37. L. D. Boni, E. L. Wood, C. Toro, and F. E. Hernandez, "Optical saturable absorption in gold nanoparticles," Plasmonics **3**(4), 171–176 (2008).
38. O. Schmidt, J. Rothhardt, F. Röser, S. Linke, T. Schreiber, K. Rademaker, J. Limpert, S. Ermeneux, P. Yvernault, F. Salin, and A. Tünnermann, "Millijoule pulse energy Q-switched short-length fiber laser," Opt. Lett. **32**(11), 1551–1553 (2007).

1. Introduction

During the last decade, nano-materials with saturable absorption property have become one of the major drivers for pulse generation in lasers [1–23]. Metal nanoparticles, an important component of these promising nano-materials, have attracted intensive attention and been widely investigated for Q-switching or mode-locking operation [16–23], mainly due to the large third order nonlinearity [24,25], broadband absorption and fast response time as a time scale of few picoseconds [16,26]. The saturable absorption property of metal nanoparticles is governed by the excitation of localized surface plasmon resonance (SPR) [27,28]. Noted that the strongly enhanced SPR of metal nanoparticles at optical frequencies makes them excellent scatterers and absorbers of visible-light [29–32], they could be an ideal candidate as visible-wavelength Q-switchers or mode-lockers. However, this type of saturable absorbers (SAs) was employed mainly in the spectral region above 1 μm [16–23]. At least to our knowledge,

#246394 Received 20 Jul 2015; revised 20 Aug 2015; accepted 21 Aug 2015; published 4 Sep 2015

performance in the short wavelength range, such as the attractive visible region, is still unproven experimentally.

With the growing applications of visible pulsed lasers in material processing, spectroscopy, medical fields and laser display, there are extremely urgent demand to practically check whether the metal nanoparticles can be used to induce visible pulsed operation or not. Gold nanoparticle (GNP), as the typical metal nanoparticle, could be preferred. Especially, GNP has large third-order nonlinear coefficient (~10^{-6} esu) when compares with the traditional nano-materials (e.g. carbon nanotube (10^{-8}~10^{-9} esu) and graphene (~10^{-7} esu)) [24,33], making it easy to obtain self-starting Q-switching or mode-locking operation as a SA. For further demonstration, the as-selected GNPs could be conventionally made into film for visible fiber lasers or deposited on glass-substrate for visible solid-state lasers. Compared to solid-state lasers, fiber lasers possess the advantages of compact, flexibility and stabilization. To construct high performance visible fiber lasers, praseodymium (Pr^{3+})-doped ZrF_4-BaF_2-LaF_3-AlF_3-NaF (ZBLAN) fibers could be applied as gain mediums because of the low maximum phonon energy (< 600 cm^{-1}) and low loss (< 0.1 dB/m) in the visible waveband as well as abundant visible transitions (e.g. blue, green, orange and red) [34]. Meanwhile, down-conversion of Pr^{3+} ions pumped by a blue GaN laser diode (LD) could enhance the laser efficiency [35]. Furthermore, dielectric film coated fiber-end has been recently proposed to fabricate fiber-compatible visible reflection mirror, which is helpful for all-fiber configuration. If the filmy GNPs SA is integrated into such a compact and high-efficiency visible fiber laser, passive Q-switching or mode-locking in the visible wavelengths might thus realize with comparative good environmental durability. Noted that the GNPs possess low damage threshold, it might largely limit their practical usage. However, the large laser output method [3] and evanescent field interaction scheme [23] have been proposed to solve this issue.

In this work, we experimentally demonstrated a GNPs-based passively Q-switched 635 nm Pr^{3+}-doped ZBLAN fiber laser. The Q-switched red fiber laser has a wide pulse-repetition-rate range of ~260 kHz and short pulse duration of 235 ns. Our results indicate that GNP is an available SA for red-light pulsed laser, revealing its potential for pulse generation in the visible region.

2. Preparation and characterization of GNPs

The GNPs used in our experiment were synthesised from the reduction of $HAuCl_4$ solution by trisodium citrate as carried in our previous report [36]. Briefly, 94 ml of water and 5 ml of 1% trisodium citrate were mixed well, and 1 ml of 1% $HAuCl_4$ was then added to the mixture. The resulting mixture was stirred and boiled in a 700 W microwave oven on high power for 1 minute, and then kept heating on medium power for 5 minutes until the color of the solution changed to wine red. The heated GNPs solution was kept at room temperature until cooled. In Fig. 1(a), the UV–Vis spectrum of the as-prepared GNPs exhibited a narrow and symmetric absorption band at 520 nm, which is attributed to the SPR band of the GNPs. And the absorption coefficient at the concerned 635 nm is about 11%. Figure 1(b) presents an X-ray diffraction (XRD) pattern of the as-synthesized products on a glass substrate. It can be seen that the diffraction peak at ca. 38.2° assigned to the {111} lattice plane of face-centered cubic (fcc) Au crystal. Figure 1(c) presents a typical TEM image of GNPs, showing spherical shape of GNPs with particle size of 15 ± 2.8 nm. Inset of Fig. 1(c) depicts the selected area electron diffraction (SAED) pattern obtained from the GNPs (Fig. 1(c)). The Scherrer ring patterns associated with the [111], [200], [220] [222], and [311] atomic planes of Au, indicating the formation of crystalline GNPs, which is in accordance with XRD pattern. Clear lattice fringes are also observed from high resolution transmission electron microscopy (HRTEM) image (Fig. 1(d)) of the GNPs with a d-spacing of 2.4 Å, which matches the expected d-spacing of the [111] plane of fcc Au (JCPDS, No. 04-0784).

For the practical usage, we dispersed the as-prepared GNPs suspension into polyving akohol (PVA) polymer with a mass concentration ratio of 40: 1, and then evaporated at 65 °C

#246394 Received 20 Jul 2015; revised 20 Aug 2015; accepted 21 Aug 2015; published 4 Sep 2015

in a drying cabinet to obtain the fiber-compatible GNPs-PVA film. To further measure the important saturable absorption parameters (e.g. modulation depth) of the GNPs in the visible region, an ultrafast visible laser source should not absent. Unfortunately, our lab has no ultrafast visible laser source, so we could not test it. However, we noticed that L. D. Boni et al. [37] have measured the optical saturable absorption of GNPs in the visible band, confirming the potential of GNPs as a visible saturable absorber.

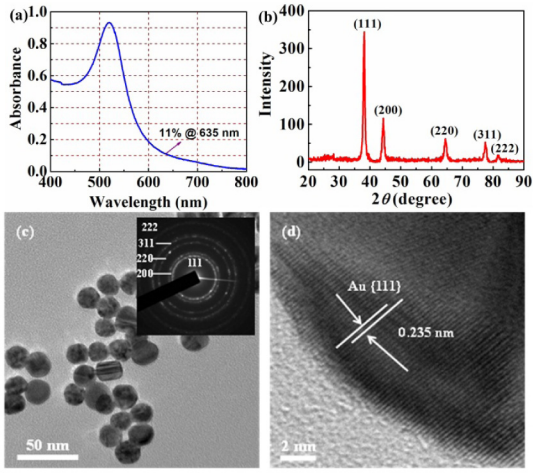

Fig. 1. (a) UV-Vis spectra, (b) XRD pattern, (c) TEM image and corresponding SAED pattern (insert), and (d) HRTEM of GNPs.

3. Experimental setup of GNPs-based passively Q-switched red Pr-doped fiber laser

The GNPs-PVA film was further incorporated into a 635 nm Pr^{3+}-doped ZBLAN fiber laser for passive Q-switching operation, as schematically shown in Fig. 2. A 444 nm/2 W GaN LD was used as the pump source. The pump light was launched into the laser cavity by a coupling system which constructed by two planoconvex lenses (PLs) and a micro-objective lens (MOL). A piece of 98.5 cm Pr^{3+}-doped ZBLAN fiber (6/125, NA of 0.15, Pr concentration 1000 ppm) was employed as the gain medium. The laser cavity with linear configuration was formed by

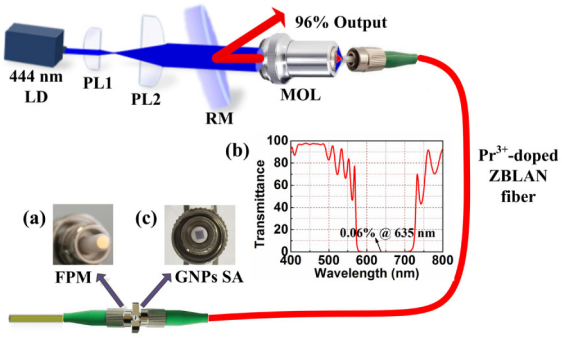

Fig. 2. Schematic illustration of the proposed GNPs-based passive Q-switching 635 nm Pr^{3+}-doped ZBLAN fiber laser, (a) the appearance of the FPM, (b) transmission spectrum of the FPM, and (c) image of the Pr^{3+}-doped fiber-end covered by filmy GNPs-PVA.

4% Fresnel reflection of a flat polishing Pr^{3+}-doped fiber-end facet and a fiber pigtail mirror (FPM) by coating high-quality dielectric films. Inset Figs. 2(a) and 2(b) respectively show the appearance and transmission spectrum of the FPM. It is a very efficient red-light all-fiber

#246394 Received 20 Jul 2015; revised 20 Aug 2015; accepted 21 Aug 2015; published 4 Sep 2015

reflector which transmits (T) only ~0.06% (i.e. reflects (R) ~99.94%) red light at 635 nm. With such a fiber-compatible reflector, the laser resonant cavity becomes rather simple and compact. The overall length of the laser cavity was about 1.97 m. The as-obtained GNPs-PVA film was placed between the FPM and the other end of the Pr fiber to form a fiber-compatible SA, as shown in Fig. 2(c). The laser was output from a red mirror (RM, T~84%@444 nm and R~99%@635 nm) which catty-cornered before the MOL. The output lasers were monitored and measured by an optical spectrum analyzer, a power meter, and an oscilloscope or a radio-frequency (RF) spectrum analyzer (Gwinstek GSP-930) together with a photodetector, respectively.

4. Experimental results and discussions

Continuous wave laser operation started when the incident pump power was increased to 113.5 mW, and stable pulse laser oscillation was achieved as soon as the incident pump power exceeded the threshold of 126.3 mW. By gradually increasing the incident pump power from 126.3 to 152.8 mW, as shown in Fig. 3, the stable pulse trains with different repetition rates were obtained, exhibiting the typical feature of passive Q-switching. Noted that SAs could be over-blanched at higher pump intensity, it may lead the pulse to be unstable. In our laser, the Q-switched pulses jittered when the pump power is over 153 mW.

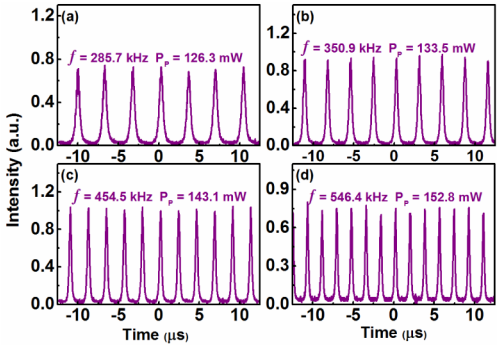

Fig. 3. The Q-switched pulse trains under different incident pump powers P_P, (a) P_P = 126.3 mW, (b) P_P = 133.5 mW, (c) P_P = 143.1 mW, and (d) P_P = 152.8 mW.

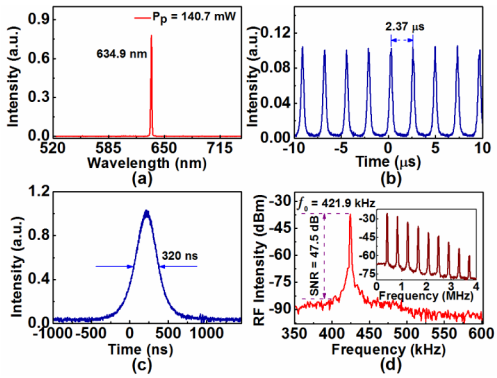

Fig. 4. The typical Q-switching characteristics of the 635 nm red fiber laser at the incident pump power of 140.7 mW, (a) output optical spectrum, (b) typical oscilloscope trace, (c) single pulse envelope, and (d) RF output spectrum. Inset: broadband RF output spectrum.

Figure 4 summarizes the typical characteristics of the Q-switching operation at an incident pump power of 140.7 mW. Figure 4(a) shows the emission spectrum of the GNPs-based Q-switched Pr^{3+}-doped ZBLAN fiber laser. The operating center wavelength is about 634.9 nm. Figures 4(b) and 4(c) respectively show the output pulse trains and single pulse profile of the

#246394 Received 20 Jul 2015; revised 20 Aug 2015; accepted 21 Aug 2015; published 4 Sep 2015

red Q-switched fiber laser. The time interval between two adjacent pulses is about 2.37 μs, corresponding to a repetition rate of ~421.9 kHz. And the pulse has a narrow full width at half maximum (FWHM) of 320 ns, which benefits from the short cavity length [38]. Figure 4(d) shows the RF spectrum of the Q-switched pulse trains. The fundamental frequency peak locates at 421.9 kHz, which coincides well with the above calculated pulse repetition rate value. The signal to noise ratio (SNR) was measured as 47.5 dB at a resolution of 30 Hz. The wide-band RF spectrum without spectral modulation was also shown in inset of Fig. 4(d). These results indicate good Q-switching stability.

In Fig. 5(a), the pulse-repetition-rate and the pulse duration as a function of the incident pump power were recorded, respectively. When gradually increases the incident pump power from 126.3 to 152.8 mW, the pulse repetition rate can be almost linearly tuned from 285.7 to 546.4 kHz. Meanwhile, the pulse duration rapidly decreases from 556 to 235 ns. The blenching speed of GNPs SA increases with the pump power, which leads to the increase of the pulse-repetition-rate and the reduction of the pulse width. Figure 5(b) draws the variation tendency curves of output power and pulse energy with the incident pump power. The output power increases linearly at first, and then becomes saturated and even decreases at higher pump power. The pulse energy increases slightly and then quickly decreases. These may be due to the quickly bleaching and the seriously thermal accumulation of the GNPs SA under high pump intensity. To exclude the thermal damage of the GNPs SA, we decreased the incident pump power and the output power can recover again, indicating no damaged of the GNPs SA. At the incident pump power of 148.0 mW, the maximum output power was measured to be 11.1 mW. And the maximum pulse energy of 27.7 nJ was obtained with the incident pump power of 133.5 mW. We believe that the higher pulse energy could be realized by further improving the quality of GNPs SA, or optimizing the cavity designs.

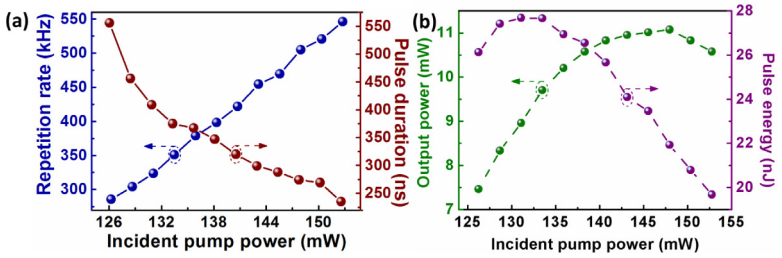

Fig. 5. (a) Repetition rate and pulse duration as a function of the incident pump power, and (b) the average output power and pulse energy as a function of the incident pump power.

5. Conclusion

In conclusion, we have successfully demonstrated that GNPs can be used to build a SA for 635 nm Q-switched pulse generation. When the SA was used in a Pr^{3+}-doped ZBLAN fiber laser, stable passively Q-switching was achieved for a tunable repetition rate range from 285.7 to 546.4 kHz and the pulse duration can be as narrow as 235 ns. The results exhibit that the GNPs film has good saturable absorption ability in the visible spectral region.

Acknowledgments

This work is supported partially by the National Natural Science Foundation of China (61275050), and partially supported by the Specialized Research Fund for the Doctoral Program of Higher Education (20120121110034).

#246394 Received 20 Jul 2015; revised 20 Aug 2015; accepted 21 Aug 2015; published 4 Sep 2015